available at www.sciencedirect.com

ScienceDirect

www.elsevier.com/locate/brainres

BRAIN RESEARCH

Research Report

Automated characterization of nerve fibers labeled fluorescently: Determination of size, class and spatial distribution

Dimiter Prodanov[a,c,*], *Hans K.P. Feirabend*[b]

[a]*Department of Physiology and Pharmacology, Catholic University of Louvain, Brussels, Belgium*
[b]*Department of Anatomy, Leiden University Medical Center (LUMC), Leiden, The Netherlands*
[c]*Bioelectronic Systems Group, NEXT Department, Interuniversity Microelectronics Center (IMEC), Heverlee, Belgium*

ARTICLE INFO

Article history:
Accepted 7 July 2008
Available online 23 July 2008

Keywords:
Fluoro-Gold
Myelinated axon topography
ImageJ
Mathematical morphology
Motor neuron
Regression tree

ABSTRACT

Morphological classification of nerve fibers could help interpret the assessment of neural regeneration and the understanding of selectivity of nerve stimulation. Specific populations of myelinated nerve fibers can be investigated by retrograde tracing from a muscle followed by microscopic measurements of the labeled fibers at different anatomical levels. Gastrocnemius muscles of adult rats were injected with the retrograde tracer Fluoro-Gold. After a survival period of 3 days, cross-sections of spinal cords, ventral roots, sciatic, and tibial nerves were collected and imaged on a fluorescence microscope. Nerve fibers were classified using a variation-based criterion acting on the distribution of their equivalent diameters. The same criterion was used to classify the labeled axons using the size of the fluorescent marker. Measurements of the axons were paired to those of the entire fibers (axons+myelin sheaths) in order to establish the correspondence between so-established axonal and fiber classifications. It was found that nerve fibers in L6 ventral roots could be classified into four populations comprising two classes of Aα (denoted $A\alpha^1$ and $A\alpha^2$), Aγ, and an additional class of Aγα fibers. Cut-off borders between Aγ and Aγα fiber classes were estimated to be 5.00±0.09 μm (SEM); between Aγα and $A\alpha^1$ fiber classes to be 6.86±0.11 μm (SEM); and between $A\alpha^1$ and $A\alpha^2$ fiber classes to be 8.66±0.16 μm (SEM). Topographical maps of the nerve fibers that innervate the gastrocnemius muscles were constructed per fiber class for the spinal root L6. The major advantage of the presented approach consists of the combined indirect classification of nerve fiber types and the construction of topographical maps of so-identified fiber classes.

* *Corresponding author*. Bioelectronic Systems Group, Interuniversity Microelectronics Center (IMEC), Kapeldreef 75, B-3001 Leuven, Belgium.
E-mail address: dimiterpp@gmail.com (D. Prodanov).

Abbreviations: ANOVA, analysis of variance; CCD, charge-coupled device; CE, coefficient of error; DAPI, 4′,6-Diamidino-2-phenylindole; FG, Fluoro-Gold; FITC, Fluorescein; GLM, General Linear Model; HRP, Horseradish peroxidase; KS, Kolmogorov–Smirnov; MM, Mathematical morphology; PF, paraformaldehyde; ROI, Region of interest; SE, Structuring Element; SEM, standard error of the mean; SD, standard deviation; SW, Shapiro–Wilk

0006-8993/$ – see front matter © 2008 Elsevier B.V. All rights reserved.
doi:10.1016/j.brainres.2008.07.049

1. Introduction

Classification of nerve fibers from a histological section can be important in studies of selective peripheral nerve stimulation by neural prostheses, neural regeneration and demyelinating disorders, among others.

In order to allow activation of only one particular bundle of motor fibers, during selective stimulation of the nerves, the intensity of the injected current should vary between certain threshold values. Since functionally-different myelinated fibers in principle have very different sizes and because the activation threshold for extraneural stimulation is inversely related to the fiber size (Blair and Erlanger, 1933), this stimulation should be size-selective. Therefore, the fiber spectrum and spatial distribution of the fibers with respect to the efferent targets of the nerves (e.g. muscles) should optimize stimulation and recording protocols.

Similarly, after a complete nerve lesion, in regenerating nerves neither the average size of the fibers in the nerve nor the electrophysiological properties of the different classes of fibers revert to their original values (Vleggeert-Lankamp et al., 2004). Since different fiber classes can follow different dynamics in their regeneration it could be of importance to describe separately the regenerating fiber populations.

Demyelinating disorders are associated with nerve fiber degeneration and axonal loss. In these conditions, the normal composition of the nerve tracts and some peripheral nerves is severely disrupted. As a result, the conduction of nerve impulses and associated sensory and motor functions are impaired (for review see Bjartmar et al., 1999). However, not all fiber types are equally affected. Therefore, it would be very useful if different fiber classes are studied separately.

Previous studies (Sima, 1974; Schmalbruch, 1986; Prodanov and Feirabend, 2007) did not address the topographic relationships between the different fiber classes throughout the course of the same nerve. An objective of the present study was to characterize the nerve fiber spectrum and the associated nerve fiber spatial distribution of the rat gastrocnemius muscles (lateral and medial) in view of their frequent use as models in regeneration (Jenq and Coggeshall, 1985; Vleggeert-Lankamp et al., 2004; Varejao et al., 2004) and neuroprosthetic (Lago et al., 2005) studies.

In whole nerves or tracts, complete semi-automatic fiber measurements, i.e. manual tracking of perimeters of fiber profiles followed by automatic measurement of the corresponding profile areas, are extremely time consuming. Therefore, they are usually abandoned in studies demanding numerous fiber measurements, like those studying nerve regeneration. Separate nerve fiber profiles are difficult to detect by computer algorithms due to their composite morphology (comprising an axon and a myelin sheath) and their close packing. Existing algorithms for fiber recognition are limited only to bright-field microscopic images (Romero et al., 2000). No automated methods are developed at present for fluorescence microscopic images. Such methods are in principle necessary, since the standard morphometric protocols for nerve fibers involve incubation in OsO_4 and curing at high temperatures, which both suppress very effectively the marker's fluorescence. Therefore, these protocols are incompatible with fluorescence labeling of structures, such as by antibodies conjugated to fluorescent molecules and fluorescent tracers.

To solve this problem, we developed an automated morphometric and analytical procedure for identification and classification of nerve fibers into anatomical sub-types. We related the size of the nerve fiber to the size of an axonal marker specific for a given sub-category of fibers. It is shown that a simple variation-based criterion could objectively classify the measured fibers into physiologically meaningful fiber classes without prior assumptions on the followed size distribution. Moreover, this classification corresponds with the classification based on the measured intra-axonal fluorescence labeling. Finally, a topographic reconstruction of the so-identified fiber classes is also produced.

2. Results

2.1. *Tracer availability in the injection site and the spinal cord motor neurons*

The injection sites in the gastrocnemius muscles were clearly discernible. The spill of tracer toward adjacent muscles was

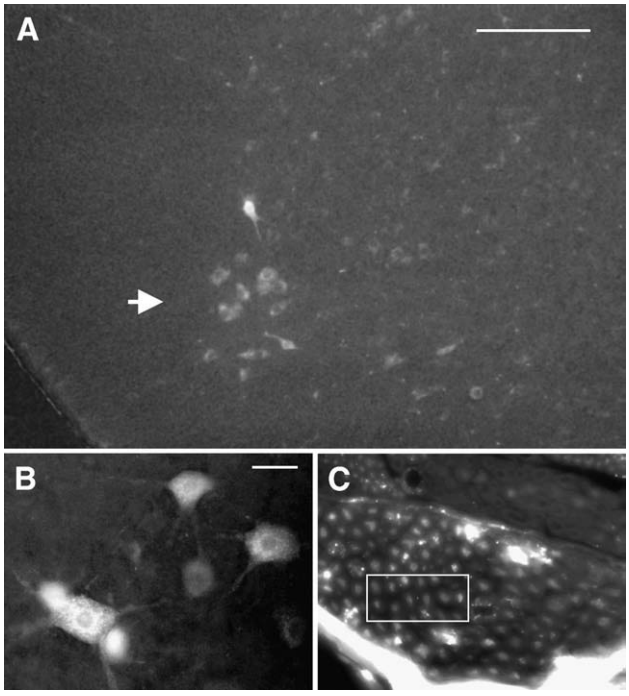

Fig. 1 – Tracing in the spinal motor neurons and peripheral nerve axons. (A) Low magnification view of the ventro-lateral part of the L6 spinal cord, Fluoro-Gold channel, scale bar — 230 μm. Fluoro-Gold-positive motor neurons are situated within Rexed lamina IX (arrow). (B) High magnification view of the Fluoro-Gold-positive motoneurons in the gastrocnemius motor nucleus, Fluoro-Gold channel, scale bar — 50 μm. The fuzzy spots are two other motoneurons that are not in the plane of focus. Fluoro-Gold is localized in the cytoplasm, while the nuclei are negative. The dendrites show less fluorescence than the somata. (C) A peripheral fascicle of the tibial nerve, Fluoro-Gold channel. Note the autofluorescent perineurium and the variation in the filling of axons. The bright fuzzy blobs are dust particles. A ROI with dimensions 71 μm × 32 μm is marked onto the image (see also Fig. 3).